

2), 334 (M^+ , 3), 287 (65), 286 (77), 285 ($M^+ - 59$, 100), 284 (93), 239 (42). Anal. Calcd for $C_{18}H_{16}O_2Cl_2$: C, 64.49; H, 4.81; Cl, 21.15. Found: C, 64.60; H, 4.79; Cl, 21.16.

Registry No. 1a, 5350-57-2; 1b, 55816-25-6; 1c, 20114-55-0; 1d, 5463-11-6; 2a, 983-79-9; 2b, 5895-68-1; 2c, 5831-42-5; 2d,

50482-89-8; 3a, 2235-01-0; 3b, 86456-47-5; 3c, 2186-93-8; 3d, 6861-53-6; 4a, 1016-09-7; 4b, 18939-92-9; 4c, 2186-95-0; 4d, 55702-41-5; 5a, 101-81-5; 5b, 4957-14-6; 5c, 726-18-1; 5d, 101-76-8; 7a, 6975-21-9; 7b, 86456-48-6; 7c, 35525-34-9; 7d, 86456-49-7; 7e, 56701-20-3; 7f, 86456-50-0; $CH_2=C(Me)COOMe$, 80-62-6; $CH_2=C(Me)CN$, 126-98-7; $CH_2=C(Me)CONH_2$, 79-39-0.

Molecular Orbital Study on the Gas-Phase Nucleophilic Displacement on Acyl Chlorides

Shinichi Yamabe* and Tsutomu Minato

Department of Chemistry, Nara University of Education, Takabatake-cho, Nara 630, Japan

Received August 17, 1982

The mechanism of the nucleophilic displacement is investigated by molecular orbital (MO) calculations. The minimum-energy paths of two gas-phase reactions, (a) $F^- + CH_3COCl \rightarrow CH_3COF + Cl^-$ and (b) $Cl^- + CH_3COCl \rightarrow CH_3COCl + Cl^-$, are sought by geometry optimization. The stable tetrahedral intermediate is not found in the reaction and the bond interchange ($X^{\cdots}CO-Cl \rightarrow X-CO^{\cdots}Cl$) takes place in the concerted fashion. The path is interpreted in terms of the frontier orbital theory. The presence or the absence of the double-well potential is discussed in relation to the basicity of X^- .

The attack of a nucleophile at a carbonyl center plays an important role in many organic and biochemical reactions, and is extensively investigated because of its contribution to the enzymatic catalysis in reactions of carboxylic acids.¹ While these studies have been made in solution, recent development of ion cyclotron resonance (ICR) spectroscopy makes it possible to observe the gas-phase ion-carbonyl compound reactions. Such solvent-free data reveal the intrinsic reactivity of the carbonyl compound which is determined solely by the electronic and structural nature of the reagent and the carbonyl substrate. The reaction is believed to proceed through the tetrahedral intermediate. Asubiojo and Brauman have argued that the tetrahedral structure is located not at the energy minimum but at the saddle point of the gas-phase reaction on the basis of kinetic data for many nucleophilic displacements.² To shed light on many disputable points for tetrahedral intermediacy in the gas phase, we present here an ab initio MO calculation for the nucleophilic displacement between a halide ion and an acetyl chloride. To our knowledge, the theoretical research of such realistic reactions has not been made, although some model reactions (e.g., $H^- + H_2C=O$ ³) were traced. The potential energy profile obtained here is compared with that deduced experimentally, and the factor of initiating the reaction is analyzed in terms of the frontier orbital theory.

Method of Calculation

The electronic structure and the minimum-energy path are investigated by the standard closed-shell SCF wave function with the 4-31G + p + p' basis set. The diffuse p and p' GTOs, of which exponents are 0.09 and 0.07, are added to the F and Cl atoms, respectively. This augmentation by the sufficiently diffuse orbitals is needed to describe the spread out electron distribution of F^- and Cl^- and to obtain the reliable total energy (E_T).⁴ The quality

Table I. Quality of the Basis Set^a

basis set	total energy (E_T) + 700, au		enthalpy change, kcal/mol
	$CH_3COCl + F^-$	$CH_3COF + Cl^-$	
exptl			-39.4 ^b
3-21G	-7.544 66	-7.751 86	-130.0
3-21G + p + p'	-7.702 49	-7.792 61	-56.5
4-31G	-10.343 08	-10.460 15	-73.5
4-31G + p + p'	-10.423 97	-10.511 06	-54.6

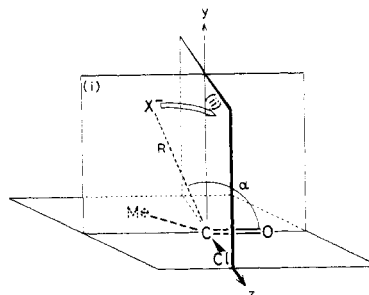
^a The geometry used in the calculation is taken from the standard value proposed by Pople. ^b Taken from ref 2.

of the basis set is indicated in Table I, in which some calculated enthalpy changes are presented and compared with the experimental data.

The geometry optimization in the course of the reaction is made in terms of the internal coordinates to the accuracy of 0.001 Å for the bond length and 0.01 degree for the angle. The GAUSSIAN 70 program is used for the present MO calculation.⁵

Results of Optimization

At the early stage of the reaction, X^- approaches the substrate from the backside of the carbonyl group in plane i as was investigated by Stone and Erskine.⁶ The stable



structure (π complex) is completed in plane i with (a) R

(1) See for instance: Patai, S., Ed. "The Chemistry of the Carbonyl Group"; Interscience: New York, 1966.

(2) Asubiojo, O. I.; Brauman, J. I. *J. Am. Chem. Soc.* 1979, 101, 3715.

(3) Bürgi, H. B.; Lehn, J. M.; Wipff, G. *J. Am. Chem. Soc.* 1974, 96, 1956.

(4) The enthalpy change of $X^-(CH_2CN)_{n-1} + CH_3CN \rightarrow X^-(CH_2CN)_n$ is well reproduced by this basis set. Yamabe, S.; Hirao, K. *Chem. Phys. Lett.* 1981, 84, 598.

(5) Hehre, W. J.; Lathan, W. A.; Ditchfield, R.; Newton, M. D.; Pople, J. A. QCPE, Indiana University, Bloomington, IN, 1973; Program No. 236.

(6) Stone, A. J.; Erskine, R. W. *J. Am. Chem. Soc.* 1980, 102, 7185.

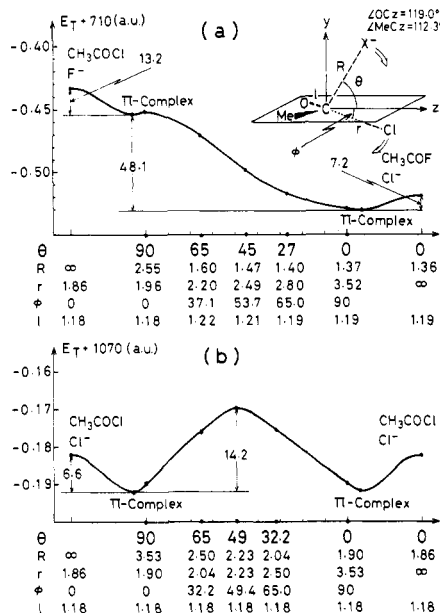


Figure 1. Potential energy profiles of (a) $\text{CH}_3\text{COCl} + \text{F}^- \rightarrow \text{CH}_3\text{COF} + \text{Cl}^-$ and (b) $\text{CH}_3\text{COCl} + \text{Cl}^- \rightarrow \text{CH}_3\text{COCl} + \text{Cl}^-$ calculated with the MO of the 4-31G + p + p' basis set. At a given θ , geometric parameters R , r , l , and ϕ are optimized. Distances R , r , and l , are in angstroms, and θ and ϕ are in degrees. It should be noted that the energy scale of the energy curve of part a is different from that of part b. The energy height is in kilocalories/mole.

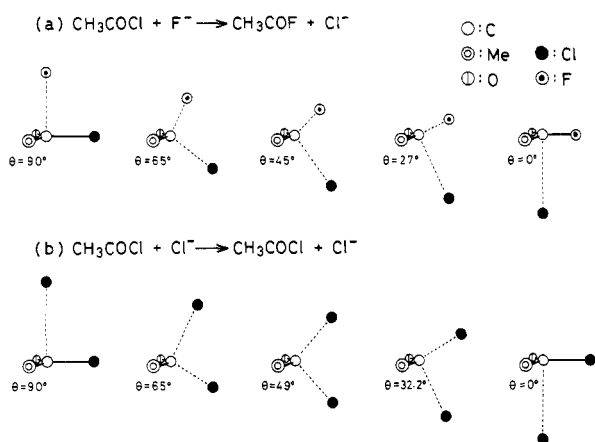


Figure 2. Snapshot of the nucleophilic displacement exhibited in the yz plane.

= 2.55 Å and $\alpha = 102^\circ$ and (b) $R = 3.53$ Å and $\alpha = 110^\circ$, respectively. For the further progress of the reaction, X^- should be shifted from plane i to plane ii as is verified in the next section. Since this deliberate shift of i \rightarrow ii at those R 's gives only ~ 1 kcal/mol destabilization, we may assume that the reaction proceeds in the yz plane.

In Figure 1 the energy profile obtained by the geometry optimization is exhibited. For two nucleophiles, $\text{X}^- = \text{F}^-$ and Cl^- , the energy curves are quite different. For $\text{X}^- = \text{F}^-$, the energy barrier brought about by the bond interchange is almost absent, which indicates clearly the large basicity of the anion. The small energy ascent (7.2 kcal/mol) is needed to decompose the loose $\text{CH}_3\text{COF} \cdots \text{Cl}^-$ π complex to $\text{CH}_3\text{COF} + \text{Cl}^-$. For $\text{X}^- = \text{Cl}^-$, the nucleophile is the same as the leaving group. The energy curve shows a typical double-well shape where two energy minima correspond to the π complexes. The bond interchange associates the energy barrier at $\theta = 49^\circ$. The moderate basicity of Cl^- may reflect such a subtle energy change in the course of the reaction. It is noteworthy that the $\text{C}=\text{O}$

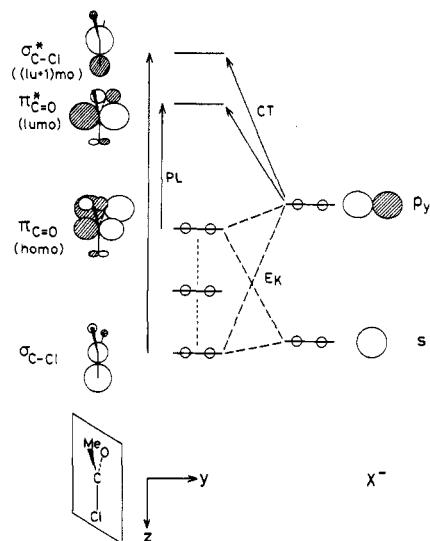


Figure 3. Schematic presentation of three orbital interactions. E_K is the exchange interaction, CT is the charge-transfer interaction, and PL is the polarization interaction.

bond (l in Figure 1) becomes only slightly longer (1.18 \rightarrow 1.22 Å) or is kept almost constant during the reaction. This demonstrates that the double bond nature is almost maintained in the nucleophilic displacement.

In Figure 2, the minimum-energy paths of a and b are sketched by the use of the geometric parameters displayed in Figure 1. The attacking halide ions [(a) F^- and (b) Cl^-] push down the leaving group through the exchange repulsion. The figure shows clearly the bond interchange of $\text{X} \cdots \text{C}-\text{Cl} \rightarrow \text{X}-\text{C} \cdots \text{Cl}$. At $\theta = 45^\circ$ (a) and $\theta = 49^\circ$ (b), the geometries similar to the tetrahedral intermediate are observed. We try to seek the structure of the intermediate with the $\text{C}-\text{O}$ bond which is regarded as their isomer. However, their optimized geometries cannot be found, because the elongation of the $\text{C}-\text{O}$ bond makes the system unstable. Thus, the well-accepted tetrahedral structure is distinctly unfavorable.

Analysis of the Displacement Path by the Frontier Orbital Theory

In this section, the displacement path obtained by the calculation is discussed in terms of the frontier orbital theory.⁷ It is well established that the theory may predict and interpret the proper steric course of chemical reactions. According to it, a reaction is regarded as an electronic interaction. The interaction between CH_3COCl and X^- may be partitioned into four chemically graspable terms: coulombic, exchange (E_K), charge transfer (CT), and polarization (PL).⁸ The coulombic term represents the classical electrostatic interaction. The last three are shown in Figure 3. E_K is the interaction between the occupied MOs and contributes to the deformation of CH_3COCl in the displacement. CT is the electron shift from the occupied MOs of X^- to the unoccupied MOs of CH_3COCl and is the origin of the $\text{C}-\text{X}$ bond formation. PL is the intramolecular electron excitation and contributes to the internal electron migration.

At the initial stage of the reaction, the π complex is formed by CT. The orientation of X^- is determined by the spatial extension of the unoccupied MOs of CH_3COCl , in particular, the lowest unoccupied MO (lumo). The lumo

(7) Fukui, K. "Theory of Orientation and Stereoselection"; Springer-Verlag: West Berlin, 1970.

(8) Fukui, K; Fujimoto, H. *Bull. Chem. Soc. Jpn.* 1968, 41, 1989.

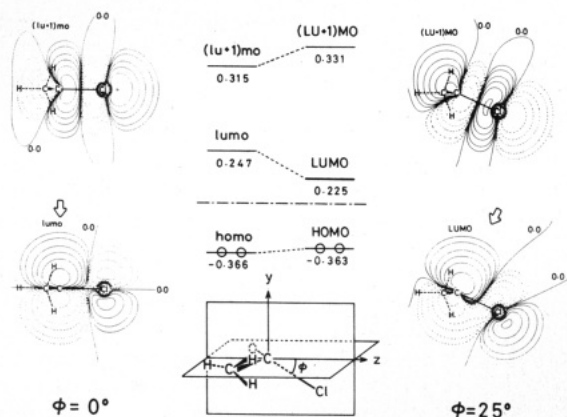
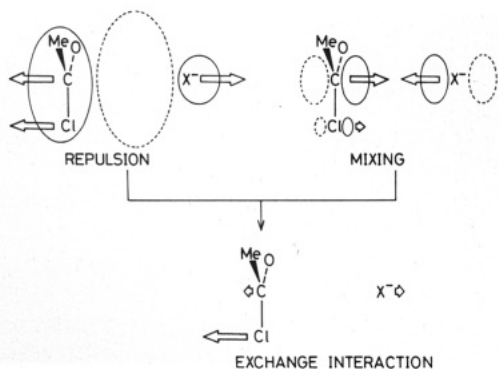


Figure 4. Change of the orbital energies and shapes by the bending of the C-Cl bond. The orbital energies of acyl chloride are in atomic units with the STO-3G basis set. HOMO and homo are the highest occupied MOs, and LUMO and lumo are the lowest unoccupied MOs. (LU + l)MO and (lu + l)mo are the second lowest unoccupied MOs. The small letters in these MO designations are for CH_3COCl of the equilibrium geometry, and the capital letters are for that of the bent-out-of-plane geometry. The values attached to contour lines in the yz plane are ± 0.2 , ± 0.1 , ± 0.07 , ± 0.05 , ± 0.02 , and ± 0.01 ($\text{e}/\text{\AA}^3$) $^{1/2}$ from inside to outer side. The empty arrow indicates the orientation of X^- based on the shapes of lumo and LUMO.

is the $\pi^*_{\text{C}=\text{O}}$ MO in the y direction. The approach of X^- to CH_3COCl in this direction forms the π complex through CT: p_y atomic orbital (AO) of $\text{X}^- \rightarrow$ lumo. As the reaction proceeds, this interaction forms the C-X bond.

The approach of X^- causes E_K which operates to bend the C-Cl bond out of the xz plane. This interaction is divided into two components, the overlap repulsion and the orbital mixing,⁹ as the following diagram shows. In

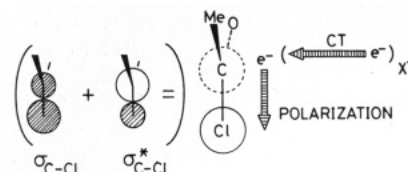


this diagram, the unbroken circle denotes the increase of electron density, and the broken circle stands for its decrease. The overlap repulsion in the left side of the figure hinders the approach of X^- by absorbing the electron density from the intermolecular region and separates the reagent from the substrate as in the case of $\text{He}\cdots\text{He}$. The orbital mixing in the right side of the figure leads to accumulation of the electron density on the carbon site of the $\text{C}\cdots\text{X}$ region. That is, $\sigma_{\text{C}-\text{Cl}}$ and $\pi_{\text{C}=\text{O}}$ MOs intermix with each other with a positive sign through the overlap with the s and p_y AOs of X^- . The carbon atom is pulled by the electron density accumulated by this orbital mixing. Thus, the cooperation of two components in E_K bends the C-Cl bond.

Next, we examine the effect of bending of the C-Cl bond on the shape and energy of the lumo. The shapes of the lumo and (lu + l)mo are illustrated in the left side of Figure

4. The term (lu + l)mo means the second lowest unoccupied MO with C-Cl antibonding character ($\sigma^*_{\text{C}-\text{Cl}}$ MO). When a deformation of $\phi = 25^\circ$ is given to the substrate as the right side of Figure 4 shows, the MO levels are found to be shifted downward and upward substantially. In particular, the LUMO composed of $\pi^*_{\text{C}=\text{O}}$ and $\sigma^*_{\text{C}-\text{Cl}}$ MOs becomes energetically lowered enough to accept the electron density of X^- . Thus, the deformation of the substrate enhances CT which further causes the lowering of the LUMO level. This cooperative acceleration (ϕ deformation vs. the energy lowering of the LUMO) is the driving force for the reaction proceeding.¹⁰ Besides the change of the MO energy, the geometric deformation brings about the mixing between $\sigma^*_{\text{C}-\text{Cl}}$ and $\pi^*_{\text{C}=\text{O}}$ MOs. When the electron density of X^- is flown into LUMO, the C-Cl bond is weakened in reflection of the antibonding nature of LUMO.

The electron migration from X^- to the leaving Cl is also explained by CT and the mixing of the occupied and unoccupied MOs of CH_3COCl . This orbital mixing corresponds to PL. The electron density, after being transferred into CH_3COCl by CT, moves from the carbonyl carbon to the leaving Cl through PL as the following diagram shows. The full and broken circles denote the



increase and decrease of electron density, respectively. $\sigma_{\text{C}-\text{Cl}}$ and $\sigma^*_{\text{C}-\text{Cl}}$ MOs intermix with each other in the opposite sign through the overlap with p_y AO of X^- .¹¹ This orbital mixing carries the electron density from C to Cl. At the initial stage of the displacement, the electron density of X^- also migrates to the oxygen atom by the mixing of $\pi_{\text{C}=\text{O}}$ MO with $\pi^*_{\text{C}=\text{O}}$ MO. However, the $\text{X}^- \rightarrow$ Cl electron migration becomes dominant as the reaction proceeds, because the deformation of CH_3COCl brings about the mixing of the $\sigma^*_{\text{C}-\text{Cl}}$ MO with the $\pi^*_{\text{C}=\text{O}}$ MO, and the $\sigma^*_{\text{C}-\text{Cl}}$ MO becomes a main component of the LUMO.

In summary, the deformation of the substrate is initiated by E_K . This geometric distortion enhances CT, both of which work cooperatively for the bond interchange. The intramolecular electron migration is induced by PL.

Single Minimum vs. Double-Well Potential

The energy barrier in the gas-phase nucleophilic displacement has been postulated in view of the kinetic data that the reaction is significantly slower than its collisional frequencies.² The absence or the presence of the energy barrier is determined by the nucleophilicity (or basicity) of the reagent ($\text{F}^- > \text{Cl}^-$). If it is larger enough (F^-) to overcome the instability of the deformation and the bond scission in the substrate, the barrier will be almost removed by the strong bond formation. If the basicity is moderate (Cl^-), the typical double-well potential should appear in the energy curve (Figure 5). The first stabilization of $\text{X}^- \cdots \text{CH}_3\text{COCl}$ is due to the π complex formation where electrons trapped in X may delocalize toward the carbonyl carbon. After the barrier is passed, the second intermediate is stabilized analogously as the CT complex. The

(9) Fujimoto, H.; Osamura, Y.; Minato, T. *J. Am. Chem. Soc.* 1978, 100, 2954.

(10) Fukui, K.; Fujimoto, H. *Bull. Chem. Soc. Jpn.* 1969, 42, 3399.
(11) Inagaki, S.; Fujimoto, H.; Fukui, K. *J. Am. Chem. Soc.* 1976, 98, 4054.

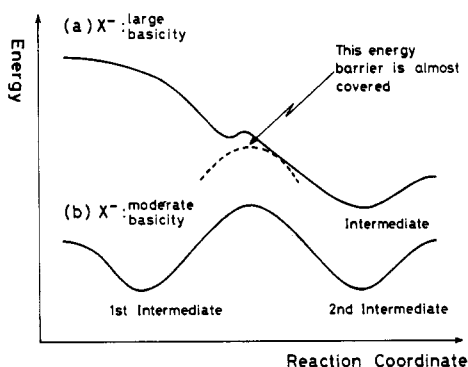


Figure 5. Double-well potential curves.

destabilization in separating the second intermediate into Cl^- and CH_3COX is the common feature in the gas-phase ion-molecule reaction.

The reactivity of trifluoro substrate CF_3COCl is compared to that of CH_3COCl . This substitution lowers the lumo and $(\text{lu} + 1)\text{mo}$ and accordingly is expected to enlarge

the rate constant of the nucleophilic displacement. In fact, $k = 1.77 \times 10^{-10} \text{ cm}^3 \text{ mol}^{-1} \text{ s}^{-1}$ for $^{37}\text{Cl}^- + \text{CF}_3\text{CO}-^{35}\text{Cl}$, whereas $k = 1.19 \times 10^{-10} \text{ cm}^3 \text{ mol}^{-1} \text{ s}^{-1}$ for $^{37}\text{Cl}^- + \text{CH}_3\text{CO}-^{35}\text{Cl}$.²

The stable tetrahedral intermediate has not been found in our calculation. In the gas phase, its possibility is determined by the criterion of whether the low-lying σ^* MO $[(\text{lu} + 1)\text{mo}]$ is available to the $\sigma^*-\pi^*$ mixing or not. For $\text{H}^- + \text{H}_2\text{C}=\text{O}$,³ CH_3O^- may be formed, because the $\sigma^*_{\text{C-H}}$ level is very high and accordingly the mixing is unlikely. The stable intermediate is merely the solvation adduct, $\text{X}^-\cdots\text{CH}_3\text{COCl}$ or $\text{Cl}^-\cdots\text{CH}_3\text{COX}$. The bond interchange shown in Figure 2 is similar to the mechanism of the $\text{S}_{\text{N}}2$ reaction where the $\text{C}=\text{O}$ bond length is kept almost constant. Like Walden inversion, the approach of X^- pushes out Cl^- in a concerted fashion.

Acknowledgment. We thank Institute for Molecular Science for the allotment of the CPU time of the HITAC M-200H computer.

Registry No. CH_3COCl , 75-36-5.

High-Yield Direct Synthesis of a New Class of Tertiary Organolithium Derivatives of Polycyclic Hydrocarbons

G. Molle, P. Bauer, and J. E. Dubois*

Institut de Topologie et de Dynamique des Systèmes de l'Université Paris VII, associé au CNRS, 75005 Paris, France

Received January 17, 1983

For the first time, 1- and 2-adamantyllithium, 1-diamantyllithium, 3,5,7-trimethyl-1-adamantyllithium, 1-twistyllithium, 3-methyl-7-noradamantyllithium, 1-triptycylolithium, and 3-homoadamantyllithium have been directly synthesized from the reaction of an organic halide and lithium metal. By use of certain experimental parameters, the phenomena at the metal-solution interface are controlled, thereby resulting in exceptionally high yields of this new class of organometallic compounds (>75%, except in the case of 3-homoadamantyllithium). Competition between formation of the organometallic compound and formation of solvent-attack byproducts is determined by the degree of adsorption of the transient species (anion radical RX^- or radical pair $\text{R}\cdot\text{Li}$) generated at the metal surface during attack by the halogenated derivative.

Unlike adamantane derivatives, which have many technological and pharmacological applications, homologous cage-structure compounds (twistane, homoadamantane, diamantane, ...) have received scant attention. One of the difficulties encountered with the latter has been the impossibility to obtain their corresponding organometallic compounds by direct synthesis.

In preceding articles,¹⁻³ we have shown that the failures encountered in synthesizing adamantyl organomagnesium compounds stemmed from poor knowledge about the phenomena occurring at the metal-solution interface during attack of the metal by the halogenated derivative. Light shed on these phenomena has enabled us to develop original methods whereby 60% yields of adamantyl organomagnesium compounds could be obtained.

Our own tests on the adamantyl organomagnesium compounds previously obtained by our methods³ give limited yields of condensation products, because condensation is sensitive to steric hindrance of the reagent. We

believed this restraint could be surmounted by using more reactive organometallic compounds.

Actually, all previous attempts at the direct synthesis of organolithium compounds^{4,5} had failed, and only the exchange $\text{R}'\text{X} + \text{RLi} \rightarrow \text{R}'\text{Li} + \text{RX}$ had resulted in a few cage-structure organolithium compounds, the first of which was 1-triptycylolithium.⁶ In previous attempts at direct syntheses using secondary or tertiary adamantyl halides and methyl or *tert*-butyllithium, tertiary⁷⁻¹⁰ and secondary^{10,11} adamantyl organolithium compounds could be obtained *only when an excess of tert-butyllithium is used*.¹² Extending this technique to 3-iodonor-

(4) Stepanov, F. N.; Baklan, V. F. *J. Gen. Chem. USSR* 1964, 34, 580.

(5) Hoek, W.; Strating, J.; Wynberg, H. *Recl. Trav. Chim. Pays-Bas* 1966, 85, 1045.

(6) Wittig, G.; Schollockopf, U. *Tetrahedron* 1958, 3, 91.

(7) Lansbury, P. T.; Sidler, J. D. *Chem. Commun.* 1965, 273.

(8) Lansbury, P. T.; Pattison, V. A.; Sidler, J. D.; Bicher, J. B. *J. Am. Chem. Soc.* 1966, 88, 78.

(9) Wieringa, J. H.; Strating, J.; Wynberg, H. *Synth. Commun.* 1972, 4, 191.

(10) Wieringa, J. H.; Wynberg, H.; Strating, J. *Tetrahedron Lett.* 1972, 2071.

(11) Wieringa, J. H.; Wynberg, H.; Strating, J. *Synth. Commun.* 1971, 1, 7.

(12) When no excess of *tert*-butyllithium was used, only dimerization hydrocarbons were obtained.^{4,8,13}

(1) Dubois, J. E.; Bauer, P.; Molle, G.; Daza, J. C. *R. Hebd. Seances Acad. Sci., Ser. C* 1977, 284C, 145.

(2) Dubois, J. E.; Molle, G.; Tourillon, G.; Bauer, P. *Tetrahedron Lett.* 1979, 5069.

(3) Molle, G.; Bauer, P.; Dubois, J. E. *J. Org. Chem.* 1982, 47, 4120.